Chapter 33

Global Analysis of Autocorrelation Functions and Photon Counting Distributions in Fluorescence Fluctuation Spectroscopy

Victor V. Skakun, Anatoli V. Digris, and Vladimir V. Apanasovich

Abstract

In fluorescence correlation spectroscopy (FCS) and photon counting histogram (PCH) analysis, the same experimental fluorescence intensity fluctuations are used, but each analytical method focuses on a different property of the signal. The time-dependent decay of the correlation of fluorescence fluctuations is measured in FCS yielding molecular diffusion coefficients and triplet-state parameters such as fraction and decay time. The amplitude distribution of these fluctuations is calculated by PCH analysis yielding the molecular brightness. Both FCS and PCH give information about the molecular concentration. Here we describe a global analysis protocol that simultaneously recovers relevant and common parameters in model functions of FCS and PCH from a single fluorescence fluctuation trace. Application of a global analysis approach allows increasing the information content available from a single measurement that results in more accurate values of molecular diffusion coefficients and triplet-state parameters and also in robust, time-independent estimates of molecular brightness and number of molecules.

Key words Fluorescence fluctuation spectroscopy, Fluorescence correlation spectroscopy, Photon counting histogram, Fluorescence intensity distribution analysis, Global analysis

1 Introduction

Fluorescence correlation spectroscopy (FCS), originally introduced by Elson et al. [1–3] in the early 1970s, has become a widely used technique for studying various dynamic molecular processes. It has found applications in measuring local concentrations, mobility coefficients, reaction rates, and detection of intermolecular interactions in vitro and in vivo [4–7]. The sensitivity and noninvasive nature of FCS has made it an important technique for studying molecular processes in cells and thus a useful tool for biochemists, biophysicists, and biologists. After developing new data analysis methods, this technique was renamed to a more general term: fluorescence fluctuation spectroscopy (FFS).

Yves Engelborghs and Antonie J.W.G. Visser (eds.), *Fluorescence Spectroscopy and Microscopy: Methods and Protocols*, Methods in Molecular Biology, vol. 1076, DOI 10.1007/978-1-62703-649-8_33,

Fluorescence fluctuation methods are based on the detection of tiny, spontaneous fluctuations in fluorescence intensity caused by deviations from thermal equilibrium in an open system. These fluctuations can arise, e.g., because of diffusion of fluorescent molecules in and out of a well-defined observation volume generated by a focused laser beam. The intensity fluctuations can be monitored and autocorrelated over time as in fluorescence correlation spectroscopy [6, 8] or a distribution of photon counts can be analyzed as in photon counting histogram (PCH) analysis [9, 10] or in fluorescence intensity distribution analysis (FIDA) [11, 12].

Performing fluorescence fluctuation spectroscopy experiments is relatively straightforward. However, the theory for FFS is based on several assumptions, which do not always hold in a real experimental situation. For example, FFS analysis assumes that the experimental observation volume has a Gaussian shape, which is not always true especially for in vivo measurements [13]. Dead time and afterpulsing of the photodetectors may influence FIDA and PCH analysis [14]. There are a number of optical factors that influence FFS measurements such as cover-slide thickness, refractive index of the sample and optical saturation that should be taken into account for proper analysis [15, 16]. In a confocal microscope configuration employing one-photon excitation, a PCH model with a three-dimensional Gaussian observation volume profile does not adequately fit the experimental fluorescence fluctuation data [17, 18]. In addition, there is a clear effect of bin time on FIDA and PCH analysis, which influences the estimation of molecular concentration and brightness [19, 20]. While it is crucial that the experimental setup must be optimized to be close to ideal conditions, one should also be aware of all these factors in the data analysis procedure to avoid erroneous fits and misinterpretation of the experimental data.

Dependence of model parameters in PCH and FIDA on the bin time makes it difficult to recover the true time-independent brightness and number of molecules from just a single measured photon counting distribution (PCD). PCD refers here to the measured and theoretical distribution of photon counts, while PCH is a commonly used term to denote the method of analysis. An attempt to fit PCD calculated at a very small bin time to avoid any influence of diffusion and triplet kinetics usually fails if the detected photon count rate is not high enough. The PCD calculated at such conditions has only a few data points, which makes it difficult to fit the data well. To get time-independent brightness and number of molecules from a fit of PCD calculated at higher bin time, knowledge of diffusion and triplet parameters is required [19, 20].

A number of extensions of PCH and FIDA methods enabling simultaneous determination of diffusion coefficients and brightness of molecules were proposed up to this time: fluorescence intensity multiple distribution analysis (FIMDA) [19], photon counting

multiple histogram (PCMH) analysis [20], master equations fluorescence intensity distribution analysis (ME-FIDA) [21], and the method, originated from the numerical solution of the diffusion equation [22].

The fit of a set of PCDs calculated at different bin times in FIMDA [19] or PCMH analysis [20] enables recovering of all parameters (including diffusion times, triplet fraction and decay time) from a single analysis. However, both FIMDA and PCMH have a drawback. These methods use the correction in the form of an integral of the time-dependent part of the FCS model. It means that the same correction value can be achieved for a different functional form of the integrand; for example, one can set the diffusion time to a very small value and compensate this by appropriate value of triplet parameters and vice versa. Therefore, after global analysis of several PCDs, the fit can be satisfactory, but results in erroneous values for diffusion, triplet, and (also) other parameters.

Although it is well possible to analyze FFS data separately by original FCS and PCH/FIDA methods or their extensions and to estimate all parameters of interest, it is advantageous to combine the complementary FFS methods in a global analysis and to increase the information content available from a single measurement. FCS has been established as a robust method for estimation of triplet parameters (fraction and decay time) and diffusion times (or coefficients) [8]. Vice versa, after correcting for the bin-time effect (using obtained estimates of triplet and diffusion parameters), PCH/FIDA analysis yields correct time-independent estimates for the brightness that finally helps to obtain correct concentrations in FCS, if the sample contains two (or more) components having different brightness values. Global analysis of ACF and PCD increases sensitivity and accuracy of the analysis while keeping the total number of fit parameters almost unchanged. Therefore, it results in more accurate values of triplet-state and diffusion parameters and also in robust, time-independent estimates of molecular brightness and number of molecules for a relatively broad range of measurement conditions.

The growing number of applications of FFS methods demands for new approaches in data processing, aiming at increased speed and robustness. Iterative algorithms of parameter estimation, although proven to be universal and accurate, require some initial guesses (IG) for the unknown parameters. If the IG are in close proximity to the optimal values of unknown parameters, they can significantly increase the efficiency and accuracy of the fit. If the target criterion surface has a complex shape with many local minima, the possibility to reach the global minimum directly depends on the quality of IG. Being an essential component of any data processing technology, IG become especially important in case of PCH/FIDA, since even with apparently reasonable, and

physically admissible but randomly chosen IG, the iterative procedure may converge to situations where for a certain combination of parameters, the PCH/FIDA model cannot be numerically evaluated [23]. Iterative fitting with generated IG proved to be more robust and at least five times faster than with an arbitrarily chosen IG [23]. It is also important that a reliable algorithm of IG generation reduces user participation and thereby leads to a more standardized and automated procedure.

In this chapter we describe the global analysis protocol of ACF and PCD. The use of the method is demonstrated through fitting of experimental fluorescence fluctuation data obtained from monomeric and dimeric forms of enhanced green-fluorescent protein (eGFP) in aqueous buffer.

2 Materials

2.1 Samples

Monomeric and dimeric eGFP were purified according to a recently described procedure [24]. The two eGFP molecules in the dimer were linked by six amino acids (GSGSGS). Purified monomeric and dimeric eGFP solutions were in 50 mM TRIS buffer (pH 8.0). For the measurements, 200-μl solutions were added to an 8-chambered cover glass (Lab-Tek, Nalge Nunc International Corp., USA). Rhodamine 110 (R110) (Invitrogen) in water was used for calibration measurements.

2.2 Instrumentation

The measurements were performed on the ConfoCor 2-LSM 510 combination setup (Carl Zeiss, Jena, Germany) detailed in [25–27]. eGFP was excited with the 488 nm line from an argon-ion laser (excitation intensity in the range 10–40 μW) focused into the sample with a water immersion C-Apochromat 40× objective lens N.A. 1.2 (Zeiss). After passing through the main beam splitters HFT 488/633, the fluorescence was filtered with a band pass 505–550 and detected with an avalanche photodiode (APD). The pinhole for confocal detection was set at 70 μm. The microscope was controlled by Zeiss AIM 3.2 software. Raw intensity fluctuation data consisting of up to 4×10^6 photons were collected from single measurements. The data collection time ranged between 30 and 120 s.

3 Methods

Global analysis of ACF and PCD is performed by the iterative least-squares method with the Marquardt-Levenberg optimization [28] (*see* details of its realization in Chapter 10 by Digris et al. in the same volume). To successfully apply it in the analysis of ACF and PCD, one has to know:

1. How to calculate the FCS model?
2. How to calculate the PCH model?
3. How to generate initial guesses for fit parameters?
4. How to perform the linking of fit parameters?
5. Which criterion to use to stop the fit?

Answers to these questions are given in the subsequent subsections.

3.1 Calculation of the FCS Model

The FCS model is calculated using the general form

$$G(\tau) = G_{\text{inf}} + X_{\text{kinetics}}(\tau) \sum_i \frac{q_{0\text{eff}\,i}^2 N_{0\text{eff}\,i}}{\left(\sum_j q_{0\text{eff}\,j} N_{0\text{eff}\,j}\right)^2} \; G_{\text{motion}\,i}(\tau), \quad (1)$$

where $G_{\text{inf}} = G(\infty)$, $N_{0\text{eff}}$ is the number of molecules in the effective volume $V_{\text{eff}} = \chi_1^2/\chi_2$, $\chi_k = \int_V [B(\mathbf{r})/B_0]^k \, \mathrm{d}V$, $q_{0\text{eff}}$ is the specific brightness of molecules (in photon counts per second per molecule), $X_{\text{kinetics}}(\tau)$ denotes a kinetic process, and $G_{\text{motion}}(\tau)$ describes the type of motion of the particles. Subscript 0 denotes that the given parameter does not depend on time. $B(\mathbf{r})$ is the brightness profile function, which is the product of excitation intensity and detection efficiency. The kinetic process and type of motion depend on the experimental conditions.

To demonstrate the application of the global analysis method, we used the model describing L independent molecular species diffusing freely in a 3D-Gaussian-shaped observation volume and undergoing singlet-triplet transitions [29]:

$$G(t) = G_{\text{inf}} + \frac{1 - F_{\text{trip}} + F_{\text{trip}} e^{-t/\tau_{\text{trip}}}}{(1 - F_{\text{trip}})\left(\sum_j q_{0\text{eff}\,j} N_{0\text{eff}\,j}\right)^2} \times \sum_{i=1}^{L} \frac{q_{0\text{eff}\,i}^2 N_{0\text{eff}\,i}}{(1 + t/\tau_{\text{diff}\,i}) \sqrt{(1 + t/a^2 \tau_{\text{diff}\,i})}}, \quad (2)$$

where F_{trip} and τ_{trip} are, respectively, the fraction and the relaxation time of molecules in the triplet state, $a = z_0/\omega_0$, ω_0 and z_0 are, respectively, the lateral and axial radii of the confocal detection volume, and τ_{diff} is the lateral diffusion time, which is related to the diffusion coefficient D_{tran} via $\tau_{\text{diff}} = {\omega_0}^2/(4D_{\text{tran}})$. All molecules are supposed to have the same triplet-state parameters.

3.2 Calculation of the PCH Model

In contrast to the FCS model, which is represented by a relatively simple equation, the PCH model does not have a closed-form solution. It is calculated by a numerical algorithm that includes several steps. Here we describe the algorithm that calculates the PCD $P(k)$ via successive convolutions of single-molecular PCD

$p^{(1)}(k)$ [9]. This algorithm allows accurately calculating the PCD using a wide range of model parameters, whereas other algorithms [11, 30] fail to calculate the model due to various numerical problems. The algorithm steps are described below (*see* **Note 1** *for details*):

1. Calculate the PCD $\tilde{P}(k) = \tilde{H}(k)/M$, where $\tilde{H}(k)$ is the measured photon counting histogram and M is the total number of bins that can be readily calculated from the histogram itself: $M = \sum_k \tilde{H}(k)$, if $\tilde{H}(k)$ decays to zero.
2. Calculate the binning correction factor $B_2(T)$ for each diffusion component as

$$B_2(T) = \frac{2}{T^2}\int_0^T (T-t)g(t)\,\mathrm{d}t, \tag{3}$$

where T is the counting time interval (bin time), $g(t)$ is a time-dependent term of the autocorrelation function in FCS

$$g(t) = \frac{1 - F_{\mathrm{trip}} + F_{\mathrm{trip}}e^{-t/\tau_{\mathrm{trip}}}}{1 - F_{\mathrm{trip}}} \frac{1}{(1 + t/\tau_{\mathrm{diff}})\sqrt{(1 + t/a^2\tau_{\mathrm{diff}})}} \tag{4}$$

and a, F_{trip}, τ_{trip}, τ_{diff} are fit parameters. The integral in Eq. 3 is calculated numerically as a sum of two integrals (from 0 to t_{br} and from t_{br} to T) by the function *qadrat* [31]. The value of t_{br} is calculated as a minimum of function: $H(t) = -(s(0) - s(t))(T - t)$, where $s(t) = (T - t)g(t)$. The minimum of function can be calculated, e.g., by the function *mimin* [31].
3. Calculate $q_{\mathrm{eff}} = q_{0\mathrm{eff}}B_2(T)$, $N_{\mathrm{eff}} = N_{0\mathrm{eff}}/B_2(T)$, where $q_{0\mathrm{eff}}$ and $N_{0\mathrm{eff}}$ are fit parameters, for each brightness component (for the sake of simplicity we omitted subscripts, which denote the component index). For a multicomponent system where each brightness component has a different molecular weight, the correction should be calculated using the proper diffusion component.
4. Calculate the single-molecular PCD $p^{(1)}(k)$, $k = 1, 2, \ldots$ for each brightness component:

$$p^{(1)}(k) = \frac{1 + F_2}{(1 + F_1)^2}\left[p_{\mathrm{G}}^{(1)}(k) + \frac{1}{k!\Theta}\sum_{n=k}^{\infty}\frac{(-1)^{n-k}(q_{\mathrm{eff}}T)^n F_n}{(n-k)!(2n)^{3/2}}\right], \tag{5}$$

where F_n, $n = 1, 2$ are instrumental out-of-focus correction parameters (F_n are fit parameters) and

$$p_{\mathrm{G}}^{(1)}(k) = \frac{1}{\Theta\sqrt{\pi}k}\int_0^{\infty}\gamma(k, q_{\mathrm{eff}}Te^{-x^2})\,\mathrm{d}x. \tag{6}$$

The incomplete gamma function $\gamma(a,x)$ is calculated as described in [32] (*gammp*) and the infinite integral is calculated as a sum of two definite integrals (from 0 to 2.4 and from 2.4 to 20). The integration limits were defined empirically by investigating the behavior of the integrand for many combinations of its parameters. The additional integral was added to ensure the acceptable accuracy of the integration if the integrand does not decay to zero at 2.4. Integration is performed numerically by the function *qadrat* [31]. The parameter Θ is varied depending on the product of q_{eff} and T. We define empirically: if($q_{\text{eff}}T < 10$) $\Theta = 1$; else if($q_{\text{eff}}T < 50$) $\Theta = 6$; else if($q_{\text{eff}}T < 100$) $\Theta = 12$; else $\Theta = 20$;

5. Calculate $p^{(1)}(0) = 1 - \sum_k p^{(1)}(k), \quad k = 1, 2, \ldots$.
6. Calculate $P(k)$ for each brightness component:

$$P(k) = \sum_{M=0}^{\infty} p^{(M)}(k)\, Poi(M, \Theta N_{\text{eff}}), \tag{7}$$

where $p^{(M)}(k) = \underbrace{p^{(1)} \otimes \cdots \otimes p^{(1)}}_{M \text{ times}}(k)$ is M-times convolution of the single-molecule PCD and $Poi(k,\eta)$ denotes the Poisson distribution with the mean value η. Do it in a recurrent way: set all elements in the array $P(k)$ to zero; at $M = 0$ calculate $Poi(0, \Theta N) = e^{-Q\,N}$ and $p^{(0)}(k) = \begin{cases} 1, & k = 0, \\ 0, & k \neq 0, \end{cases}$ multiply results, and add the product to the sum; at $M = 1$ calculate $Poi(1, \Theta N) = Poi(0, \Theta N) \times \Theta N$, multiply the result to $p^{(1)}(k)$, and add the product to the sum; at $M = 2, 3, \ldots$ calculate $Poi(M, \Theta N) = Poi(M-1, \Theta N) \times \Theta N / M$, perform a convolution $p^{(M)}(k) = p^{(M-1)}(k) \otimes p^{(1)}(k)$, multiply the results, and add the product to the sum. Stop the calculation of the sum when $Poi(M, \Theta N) < 10^{-8}$ after reaching its maximum. Such recurrent calculation of both Poisson distribution and M-times convolution increases the computation efficiency of the algorithm.
7. Calculate the total PCD. The PCD of a number of independent species is given by a convolution of PCD of each species

$$P(k) = P(k, N_{\text{eff}\,1}, q_1) \otimes \cdots \otimes P(k, N_{\text{eff}\,n}, q_n). \tag{8}$$

8. Perform the final convolution of the obtained $P(k)$ with the background term

$$P(k, \lambda) = P(k) \otimes Poi(k, \lambda T), \tag{9}$$

where λ is the background count rate (fit parameter), if necessary.
9. Perform the correction on afterpulses and dead time if necessary. Correction on afterpulses and dead time can be made

according to the algorithm described in [21]. Correction for afterpulses is done by the following formula:

$$P_{\text{AP corr}}(k) = \sum_{j=0}^{m} P_0(k-j)\, P_{\text{binomial}}(j; k-j, p_{\text{ap}}), \tag{10}$$

where p_{ap} is the afterpulsing probability, m is a number of points in PCD, $P_0(k)$ is the ideal PCD (i.e., without the correction), and P_{binomial} is the binomial distribution

$$P_{\text{binimial}}(j; M, p) = \frac{M!}{j!(M-j)!} p^j (1-p)^{M-j}, \quad j = 0, 1, \ldots, M. \tag{11}$$

This algorithm works well, if afterpulses are always counted in the same bin together with the main events. This assumption is satisfied for avalanche photodiodes where afterpulses are delayed on a relatively short time (25–40 ns). Correction for dead time is done by the following formula:

$$P_{\text{DT corr}}(k) = \sum_{j=0}^{\infty} P_0(k+j) P_{\text{binomial}}\left(j; k+j, \frac{(k+j)\tau_{\text{dt}}}{T + (k+j)\tau_{\text{dt}}}\right), \tag{12}$$

where τ_{dt} is the detector dead time. Parameters p_{ap}, τ_{dt} are fit parameters.

3.3 Generation of Initial Guesses in Photon Counting Histogram Analysis

Here we describe the efficient algorithm of generation of initial guesses for "main" parameters ($q_{0\text{eff}\,i}$ and $N_{0\text{eff}\,i}$, $i = 1,2$ and F_1, F_2) of one- and two-component PCH models:

1. Calculate the first four cumulants $\tilde{K}_n$ of the measured PCD. The experimental fluorescence factorial cumulants are calculated through fluorescence factorial moments $\tilde{F}_n$

$$\tilde{K}_n = \tilde{F}_n - \sum_{i=1}^{n-1} \frac{(n-1)!}{i!(n-i-1)!} \tilde{K}_{n-i} \tilde{F}_i, \tag{13}$$

$$\tilde{F}_n = \langle (k-1)\ldots(k-n+1) \rangle = \sum_{k=n}^{m} k(k-1)\ldots(k-n+1)\tilde{P}(k), \tag{14}$$

where $\tilde{P}(k)$ is a measured PCD and the angular brackets indicate averaging with the set of probabilities $\tilde{P}(k)$. If a photon counting histogram $\tilde{H}(k)$ is measured instead of PCD $\tilde{P}(k)$, one must perform the normalization: $\tilde{P}(k) = \tilde{H}(k)/M$.

2. For the case of a one-component model, calculate IG using equations summarized in Table 1 (*see* **Note 2** *for details*).
3. Calculate $B_2(T)$ as described in Subheading 3.2, **step 2**.

Table 1
Initial guesses for PCH analysis for a one-component system

Parameter fixing	IG
λ, F_1, F_2 are fixed	$N_{\text{eff}} = \frac{(\tilde{K}_1 - \lambda T)^2}{\tilde{K}_2}$, $q_{\text{eff}} = \frac{(1+F_1)\tilde{K}_2}{\gamma_2(1+F_2)(\tilde{K}_1 - \lambda T)T}$
F_1, F_2 are fixed	$N_{\text{eff}} = \frac{\gamma_3^2(F_1+1)^2\tilde{K}_2^3}{\gamma_2^4(F_2+1)^4\tilde{K}_3^2}$, $q_{\text{eff}} = \frac{\gamma_2(1+F_2)\tilde{K}_3}{\gamma_3\tilde{K}_2 T}$, $\lambda = \frac{\tilde{K}_1}{T} - \frac{\gamma_3(F_1+1)\tilde{K}_2^2}{\gamma_2^2(F_2+1)^2\tilde{K}_3 T}$
λ, F_1 are fixed	$N_{\text{eff}} = \frac{(\tilde{K}_1 - \lambda T)^2}{\tilde{K}_2}$, $q_{\text{eff}} = \sqrt{\frac{(1+F_1)\tilde{K}_3}{\gamma_3(\tilde{K}_1 - \lambda T)}}$, $F_2 = \frac{\tilde{K}_2\sqrt{\gamma_3(1+F_1)}}{\gamma_2\sqrt{\tilde{K}_3(K_1 - \lambda)}} - 1$
λ, F_2 are fixed	$N_{\text{eff}} = \frac{(\tilde{K}_1 - \lambda T)^2}{\tilde{K}_2}$, $q_{\text{eff}} = \frac{\gamma_2(1+F_2)\tilde{K}_3}{\gamma_3\tilde{K}_2 T}$, $F_1 = \frac{\gamma_2^2(F_2+1)^2\tilde{K}_3(K_1 - \lambda T)}{\gamma_3\tilde{K}_2^2} - 1$
λ is fixed	$N_{\text{eff}} = \frac{(\tilde{K}_1 - \lambda T)^2}{\tilde{K}_2}$, $q_{\text{eff}} = \frac{\gamma_3\tilde{K}_4}{\gamma_4\tilde{K}_3 T}$, $F_1 = \frac{\gamma_3^3\tilde{K}_4^2(\tilde{K}_1 - \lambda T)}{\gamma_4^2\tilde{K}_3^3} - 1$, $F_2 = \frac{\tilde{K}_2\tilde{K}_4\gamma_3^2}{\tilde{K}_3^2\gamma_2\gamma_4} - 1$

4. Calculate the time-independent estimates of brightness and number of molecules: $q_{0\,\text{eff}\,i} = q_{\text{eff}\,i}/B_2(T)$, $N_{0\,\text{eff}\,i} = N_{\text{eff}\,i}B_2(T)$. Do it independently for each brightness component using diffusion parameters from the proper diffusion component.
5. For a two-component model with known background λ and known instrumental parameters F_1, F_2, the system of nonlinear equations (Eq. 37) (*see* **Note 2** *for details*) can be reduced to a third-order polynomial with respect to $q_{\text{eff}\,2}$

$$\begin{aligned}(A_2^3A_3 - A_3^2A_1)q_{\text{eff}\,2}^3 + (2A_1A_3A_4 - A_2^2A_4 - A_2A_3^2)q_{\text{eff}\,2}^2 \\ + (A_3^3 - A_1A_4^2)q_{\text{eff}\,2} + (A_4^2A_2 - A_3^2A_4) = 0,\end{aligned} \tag{15}$$

where

$$\begin{aligned}A_1 &= (1+F_1)(\tilde{K}_1 - \lambda T)/\gamma_2(1+F_2)T, \\ A_2 &= (1+F_1)^2\tilde{K}_2\Big/\gamma_2^2(1+F_2)^2T^2, \\ A_3 &= (1+F_1)^2\tilde{K}_3/\gamma_2\gamma_3(1+F_2)T^3, \\ A_4 &= (1+F_1)^2\tilde{K}_4/\gamma_2\gamma_4(1+F_2)T^4.\end{aligned} \tag{16}$$

The gamma factors γ_n in Eq. 16 are calculated as follows (for a 3D Gaussian profile):

$$\gamma_n = \chi_n/\chi_1 = 1\big/n^{3/2}. \tag{17}$$

Seeking roots of the polynomial can be done numerically as described in [32]. The estimates of other parameters are calculated as

$$N_{\text{eff}\,2} = \frac{A_2A_4 - A_3^2}{A_2q_{\text{eff}\,2}^4 - 2A_3q_{\text{eff}\,2}^3 + A_4q_{\text{eff}\,2}^2}, \tag{18}$$

$$q_{\text{eff }1} = \frac{A_2 - N_{\text{eff }2} q_{\text{eff }2}^2}{A_1 - N_{\text{eff }2} q_{\text{eff }2}}, \qquad N_{\text{eff }1} = \frac{A_1 - N_{\text{eff }2} q_{\text{eff }2}}{q_{\text{eff }1}}. \quad (19)$$

Since in this case a number of IG is available (*see* **Note 2**), we developed a procedure of their selection. To select the best set of IG, do the following:

(a) Reject the IG that are physically unacceptable or residing outside predefined margins.

(b) Calculate the χ^2 criterion for remaining sets of IG. Set χ^2 to the largest floating value if calculation of the theoretical $P(k)$ has failed due to any reason or no roots have been found.

(c) Search the obtained matrix for IG with minimal χ^2.

Finally, apply bin-time correction as described in **steps 3** and **4**.

6. For a two-component model with known background and unknown instrumental parameters, perform the following steps:

(a) Subdivide an acceptable range of instrumental parameters F_1 and F_2 (e.g., estimated from a calibration measurement) into a number of sections.

(b) For each pair of F_1 and F_2, find the IG as described in **step 5** (without **step c**).

(c) Search the obtained matrix for the IG with minimal χ^2.

3.4 The Protocol of Global Analysis of ACF and PCD

Global analysis of ACF and PCD is demonstrated through fitting of experimental fluorescence fluctuation data obtained from monomeric and dimeric forms of enhanced green-fluorescent protein (eGFP) in aqueous buffer. Measured data used in the analysis were acquired as described in Subheading 2 and were stored in raw binary data files. Analysis is performed by the FFS Data Processor 2.3 package [33]:

1. Calculate the ACF and several PCDs. The global analysis of ACF and PCD allows extraction of time-independent values for brightness and concentration for molecular samples using just a single PCD and a single ACF. However, taking into account that PCD usually has a low number of data points, it is advisable to calculate several PCDs to increase the brightness information content of experimental data. We calculated the ACF and two PCDs from raw data with bin times of 0.2 μs, 40 μs, and 120 μs, respectively. The choice of bin times for calculation of PCDs depends on the count rate. The bin time should not be too short where the PCD has just a few data points and too long where the PCD tends to obtain a Gaussian shape.
2. Calculate weighting factors [34] of ACF and PCDs. Weighting factors of the ACF are calculated by the algorithm proposed by Wohland et al. [35]. The intensity trace is subdivided into

a number of non-overlapping sub-traces and the local autocorrelation function is calculated from each sub-trace. Then the standard deviations for each point of the ACF are obtained from these local autocorrelation functions. Finally, weighting factors of the ACF are calculated by dividing the obtained deviations by the square root of the number of sub-traces. This algorithm does not depend on the type of the ACF time scale (quasi-logarithmic or linear) and FCS model parameters (i.e., it does not require any prior knowledge about the explored system) and usually results in good estimates of standard deviations of the ACF. Weighting factors of the PCD are calculated as standard deviations of a binomial distribution given by the following: $\sigma_k = \sqrt{mp_k(1-p_k)}$, where m is the total number of bins and $p_k = \tilde{P}(k)$.

3. Fit the ACF to the FCS model (Eq. 2) in order to get proper initial values for the parameters F_{trip}, τ_{trip}, $\tau_{\text{diff } i}$, a, and G_{inf}. Performing the preliminary analysis of ACF is advisable, because IG for the bin-time correcting parameters F_{trip}, τ_{trip}, $\tau_{\text{diff } i}$, and a of the PCH model (*see* Eqs. 3 and 4) are not calculated. Initial guesses for these parameters cannot be obtained from a separate PCD. Although they can be estimated from a set of PCDs (with a number greater than or equal to the number of estimated parameters), their quality will be low if the number of PCDs included in the analysis is not high enough (as compared to the number of points in ACF). It was found that the global analysis of some PCDs (as well as some PCDs and one or several ACF together) started from arbitrary IG are often trapped in local minima due to the integral form of the applied correction [33]. Therefore, starting the global fit from nearly optimal values of F_{trip}, τ_{trip}, $\tau_{\text{diff } i}$, a, and G_{inf} prevents the analysis from trapping in local minima and increases its stability.
4. Fix F_{trip}, τ_{trip}, $\tau_{\text{diff } i}$, and a to obtained values. This step is mandatory for the FFS Data Processor because the data processor averages fit parameter values during the parameter linkage, unless at least one parameter included in the group is not fixed to some value.
5. Add PCDs to the analysis, configure the PCH model by setting on the diffusion and triplet correction, and form parameter groups. The parameters $N_{0\text{eff } i}$, $q_{0\text{eff } i}$, F_{trip}, τ_{trip}, $\tau_{\text{diff } i}$, and a should be linked across all models (FCS and PCH) and F_1, F_2 across the PCH models. If one is going to correct the PCH model for dead time and afterpulses, two additional parameter groups can be formed.
6. Generate IG for $N_{0\text{eff } i}$, $q_{0\text{eff } i}$, F_1, F_2 as described in Subheading 3.3.

Table 2
Initial guesses and best fit results of global analysis of autocorrelation function (ACF) and two-photon counting distributions (PCDs) of monomeric and dimeric eGFP

Parameter	eGFP monomer IG	eGFP monomer best fit	eGFP dimer IG	eGFP dimer best fit
F_1	0.77	0.60 ± 0.03	0.79	0.65 ± 0.01
F_2	0.079	0.037 ± 0.007	0.070	0.037 ± 0.003
a	5.0 (fixed)	5.0 (fixed)	5.0 (fixed)	5.0 (fixed)
F_{trip}	0.16	0.16 ± 0.01	0.12	0.12 ± 0.02
τ_{trip} (μs)	3.84	3.80 ± 0.56	2.23	2.29 ± 0.37
τ_{diff} (μs)	62.9	62.7 ± 0.52	96.94	97.0 ± 0.45
$N_{0\text{eff}}$	1.604	1.609 ± 0.008	1.70	1.70 ± 0.004
$q_{0\text{eff}}$ (cpsm)	38,410	54,140 ± 670	66,990	95,380 ± 580
q (cpsm)		34,990		59,810
χ^2_{gl}		0.99		1.31
$\chi^2_{\text{gl mod}}$		1.05		1.68

ACF was calculated with bin time 0.2 μs. PCD's were calculated with bin times of 40 and 120 μs. The data consisted of 1.2×10^6 photons for eGFP monomer and 2.2×10^6 photons for eGFP dimer. Initial guesses and best fit results and both χ^2 global criteria, standard and modified, are presented for comparison. Confidence intervals at the 67 % confidence level were calculated by the asymptotic standard-errors method as described in [40]. The true value of the brightness q was calculated via Eq. 41 (*see* **Note 3**)

7. Perform the iterative fit. Calculate the FCS model as described in Subheading 3.1. Calculate the PCH model as described in Subheading 3.2. Calculate the global χ^2 criterion as described in **Note 4**.
8. Unfix parameters F_{trip}, τ_{trip}, $\tau_{\text{diff }i}$, and a.
9. Perform the iterative fit again. **Step 8** can be done directly after **step 6** if you are sure that IG for all parameters were generated accurately. **Step 9** can be omitted then.

Analysis results of monomeric and dimeric eGFP are summarized in Table 2. Graphical results are shown in Fig. 1 (monomeric eGFP) and Fig. 2 (dimeric eGFP). The PCH model was calculated using Eqs. 5–7. The FCS model was calculated by Eq. 2. Parameter G_{inf} was fixed to unity, parameter λ was fixed to zero, and parameter a was fixed to the value obtained from the calibration measurement (Rho 110 in water). Although parameters F_1, F_2 are descriptive parameters of the used setup, we did not fix them to the value obtained from the calibration measurement, as even small deviations of these parameters from the best-fit value will affect the resulted PCD substantially. It is a consequence of the high sensitivity of the PCH model to the value of correction

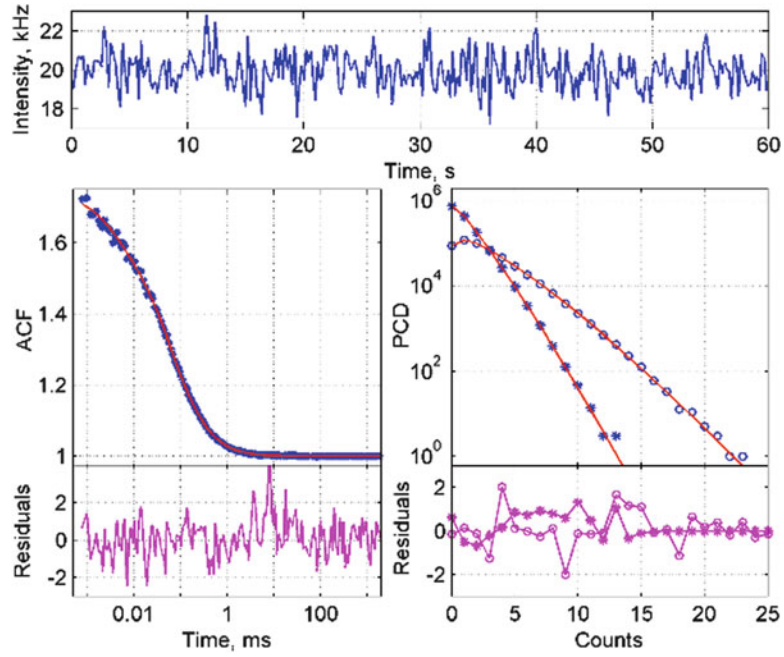

Fig. 1 Results of global analysis of autocorrelation function (ACF) and photon counting distributions (PCDs) of monomeric eGFP. PCD's were calculated with bin times of 40 μs (*closed circles*) and 120 μs (*open circles*). The experimental intensity fluctuations are shown on *top*. Residuals are plotted below each curve. Recovered parameters and criterion values are presented in Table 2

parameters F_1 and F_2. Therefore, it is advisable to link these correction parameters in the global analysis of several measurements only if they do not differ much. Initial guesses, generated by the algorithm described in Subheading 3, are presented for comparison. Analysis, being performed on a typical personal computer (Intel Core 2 Duo 2 GHz, 2 Gb RAM), lasted not more than a few seconds. After inspection of the analysis results, we can conclude that the global analysis of ACF and PCD fits the experimental data well. Brightness values and diffusion times were recovered with a good precision as indicated by calculated confidential intervals.

We obtained the ratio of the dimer and monomer brightness equal to 1.71, which is less than the expected value of 2. This can be explained by the presence of resonance energy transfer in dimeric eGFP [33, 36]. From the obtained ratio of the diffusion times (τ_{diff}) for monomeric and dimeric eGFP (0.646, expected value is 0.707), we concluded that eGFP move like rodlike molecules, which is in excellent agreement with the results of recent FCS experiments on eGFP oligomers [37].

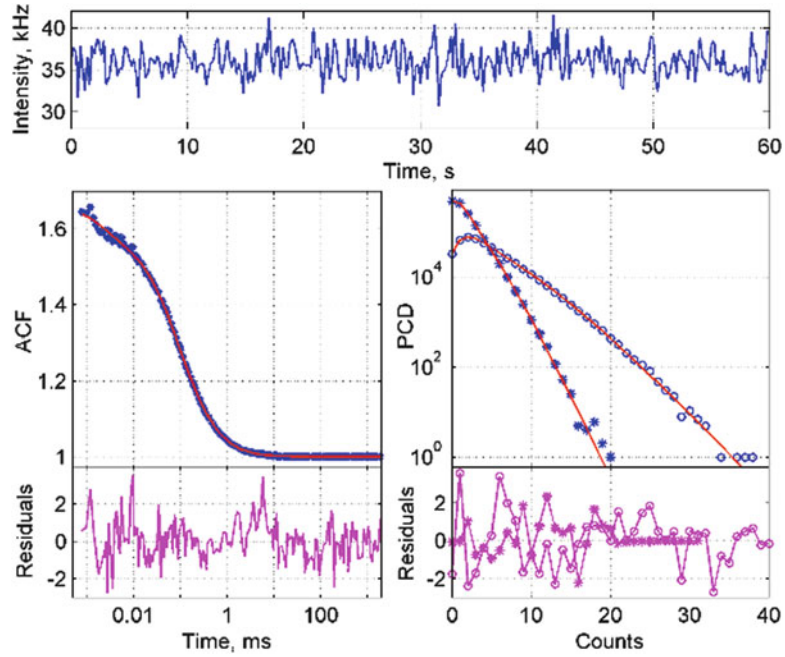

Fig. 2 Results of global analysis of autocorrelation function (ACF) and photon counting distributions (PCDs) of dimeric eGFP. PCD's were calculated with bin times of 40 μs (*closed circles*) and 120 μs (*open circles*). The experimental intensity fluctuations are shown on *top*. Residuals are plotted below each curve. Recovered parameters and criterion values are presented in Table 2

4 Notes

1. *Theory of photon counting histogram analysis*
   In PCH the total PCD from a number of molecules located in the closed volume V_0 is calculated by successive convolutions of single-molecule PCDs [9]

$$p_{V_0}^{(1)}(k) = \frac{1}{V_0} \int_{V_0} Poi(k, qTB(\mathbf{r}))\mathrm{d}\mathbf{r}, \tag{20}$$

   where $p^{(1)}(k)$ denotes a single-molecule PCD and Poi(k,η) denotes the Poisson distribution with the mean value η. The brightness q is defined as $q = I_0\sigma_a Q\kappa$, where I_0 is the excitation intensity in the focus σ_a and Q are molecular absorption cross section and fluorescence quantum yield, respectively, and κ is the detection efficiency of the confocal setup. It is assumed that the contribution of each single molecule to the recorded photon trace is independent and the emission intensity is constant during the counting time interval T. $B(\mathbf{r})$ is assumed to be a 3D Gaussian

$$B(\mathbf{r}) = B_0 \exp[-2(x^2 + y^2)/\omega_0^2 - 2z^2/z_0^2] \tag{21}$$

with $B_0 = B(0)$. To reduce the three-dimensional integral in Eq. 20 to a one-dimensional integral, let us apply the following transformation of the coordinate system:

$$\begin{cases} x = r\omega_0 \cos\varphi \sin\alpha \\ y = r\omega_0 \sin\varphi \sin\alpha \\ z = z_0 r \cos\alpha \end{cases} \tag{22}$$

where r is the length of the radius vector and φ and α are angles. The Jacobian of this transformation is

$$\partial(x, y, z)/\partial(r, \varphi, \alpha) = \omega_0^2 z_0 r^2 \sin\alpha. \tag{23}$$

Equation 21 simplifies to

$$B(r) = B_0 e^{-2r^2}, \quad r = \sqrt{x^2/\omega_0^2 + y^2/\omega_0^2 + z^2/z_0^2}. \tag{24}$$

The size of the volume V_0 with given radius r_0 depends on w_0, z_0

$$V_0 = \int_0^{r_0} \int_0^{2\pi} \int_0^{\pi} r^2 \omega_0^2 z_0 \sin\alpha \, \mathrm{d}r \, \mathrm{d}\varphi \, \mathrm{d}\alpha = \frac{4\pi}{3} r_0^3 \omega_0^2 z_0. \tag{25}$$

After integration over φ and α, Eq. 20 takes the form

$$\begin{aligned} p_{V_0}^{(1)}(k) &= \frac{4\pi\omega_0^2 z_0}{V_0 k!} \int_0^{r_0} \left(q_{\mathrm{eff}} T \, e^{-2r^2}\right)^k e^{-q_{\mathrm{eff}} T e^{-2r^2}} r^2 \, \mathrm{d}r \\ &= \frac{3}{r_0^3 k!} \int_0^{r_0} \left(q_{\mathrm{eff}} T e^{-2r^2}\right)^k e^{-q_{\mathrm{eff}} T \, e^{-2r^2}} r^2 \, \mathrm{d}r \end{aligned}, \tag{26}$$

where we define $q_{\mathrm{eff}} = B_0 q$. Note that the obtained probability distribution is normalized: $\sum_k p_{V_0}^{(1)}(k) = 1$ for any r_0. In FFS the observation volume is open and the effective size is usually estimated as $V_{\mathrm{eff}} = \chi_1^2/\chi_2$. When the observation volume is open, the choice of r_0 is crucial. The size of V_0 grows proportionally to r_0^3. Therefore, the number of molecules in this volume and consequently the number of convolutions needed for calculation of the total PCD grow very rapidly making the algorithm inefficient. The radius length must be taken as less as possible so that it completely covers the region where molecules are excited and emit photons.

The integrand in Eq. 26 decays rapidly with increasing of r_0 for any $k > 0$. It allows to set the upper integration limit in Eq. 26 to infinity and to calculate Eq. 26 in a more efficient way [9] through the incomplete gamma function $\gamma(a, x) = \int_0^x e^{-t} t^{a-1} \, \mathrm{d}t$

$$p^{(1)}(k) = \frac{3}{4r_0^3 k}\int_0^\infty \gamma(k, q_{\text{eff}}Te^{-x^2})\mathrm{d}x, \quad k = 1, 2, \ldots, \tag{27}$$

$$p^{(1)}(0) = 1 - \sum\nolimits_k p^{(1)}(k), \quad k = 1, 2, \ldots. \tag{28}$$

The photon counting distribution $P(k)$ of a number of molecules of concentration C in an open observation volume of size V_0 is the weighted average of $p^{(1)}(k)$ [9]

$$P(k) = \sum_{M=0}^{\infty} p^{(M)}(k)\, Poi(M, V_0 C), \tag{29}$$

where

$$p^{(M)}(k) = \underbrace{p^{(1)} \otimes \cdots \otimes p^{(1)}}_{M \text{ times}}(k), \quad p^{(0)}(k) = \begin{cases} 1, & k = 0, \\ 0, & k \neq 0. \end{cases} \tag{30}$$

Single-molecular PCD (*see* Eq. 25) depends on unknown parameters ω_0 and z_0. To eliminate unknown parameters, let us replace the product $V_0 C$ by $V_0 N_{\text{eff}}/V_{\text{eff}}$ in the equations above and introduce a ratio $\Theta = V_0/V_{\text{eff}} = 4r_0^3/3\sqrt{\pi}$. It results in Eqs. 6 and 7.

It was found that the value of Θ needed for accurate calculation of $P(k)$ depends on the product of $q_{\text{eff}}T$. For small $q_{\text{eff}}T$ (less than 10), it can be safely set to unity, while for greater $q_{\text{eff}}T$ it must be large enough to completely include the observation volume. This is necessary to keep the probability distribution $P(k)$ normalized for any q_{eff} and T. The dependence of Θ on $q_{\text{eff}}T$ can be explained as follows. The effective volume has a fixed size. It depends only on ω_0 and z_0 and does not depend on excitation intensity and molecular brightness. However, the illuminated volume grows with an increase of I_0. As q_{eff} and T are presented in a product in the model, the increase of binning time has the same effect.

The PCD of a number n of independent species is given by a convolution of PCDs of each species (*see* Eq. 8). Correction for the background with mean count rate λ can be done by additional convolution with Poisson distribution with parameters λT; *see* Eq. 9.

Derived expressions often fail to fit experimental data using one-photon excitation due to the large deviation of the actual brightness profile from an assumed 3D Gaussian approximation [11, 18]. To improve the model, Perroud, Huang, and coworkers [17, 18] introduced additional fitting parameters F_n defined as the relative difference between the integral χ_n of the nth power of the normalized-to-unity, actual brightness profile function $B(\mathbf{r})$, and that of its 3D Gaussian approximation $\chi_{\text{G}\,n}$.

$$F_n = (\chi_n - \chi_{G\,n})/\chi_{G\,n}. \tag{31}$$

Introducing F_n into the single-molecule PCD leads to Eq. 5 [18] where $p_G^{(1)}(k)$ is calculated by Eq. 6. In most cases only the first-order correction (all F_n equal to zero except F_1) is sufficient to get the best fit to the experimental data.

The PCH model was derived under the assumption that the fluorescence intensity emitted by a molecule during bin time T is constant, which is valid for the limit of short bin times. At arbitrary bin times, both brightness and number of molecules become a function of T. The most practical way to calculate the time-independent brightness and number of molecules is to make the first and second factorial cumulants of PCD exact [19, 20]. According to this theory one has to calculate the so-called binning correction factor [19, 20] (*see* Eqs. 3 and 4) and to correct the brightness and the number of molecules in the following form:

$$\begin{aligned} q_{0\,\mathrm{eff}} &= q_{\mathrm{eff}}/B_2(T), \\ N_{0\,\mathrm{eff}} &= N_{\mathrm{eff}}B_2(T), \end{aligned} \tag{32}$$

where $q_{0\mathrm{eff}}$ and $N_{0\mathrm{eff}}$ are absolute values of brightness and concentration that are independent on T. In general, the binning correction factor can be calculated assuming two or even more diffusing components (such correction can be applied to a mixture of species with approximately equal brightness values but quite different hydrodynamic radii). For a model of multiple brightness components, this correction has to be applied independently to each component. Triplet and diffusion characteristics can be either different or the same for each brightness component.

Although the theories of FCS and PCH/FIDA are well known, several important points have to be taken into consideration when both theories are combined in a global analysis. From the PCH/FIDA side, there are two major points. First, a correction must be applied for out-of-focus emission, which can be done by either a correction of the Gaussian profile via Eq. 31, or using a polynomial profile [11, 19]. Second, PCH/FIDA must be corrected for dynamic processes enabling to obtain time-independent estimates of brightness values and number of molecules. From the FCS side the correction on difference in brightness values must be applied when multiple fluorescent species are present. The last important point is to use the same reference volume in both FCS and PCH/FIDA. The use of the effective volume V_{eff} is preferable, because it allows linking the number of molecules (N) through FCS, PCH, and FIDA models.

2. *Theory of initial guesses for photon counting histogram analysis*
The algorithm of initial guesses is based on the statistical method of moments. The method of moments [38] is widely used in statistics to estimate parameters for any probability distribution, for which the necessary amount of moments can be generated. According to this method the theoretically obtained moments $M_n = M_n(\eta_1, \eta_2, \ldots, \eta_m)$ are equalized to the experimentally obtained ones: $\tilde{M}_n$:

$$M_n(\eta_1, \eta_2, \ldots, \eta_m) = \tilde{M}_n, \quad n = 1, 2, \ldots, m, \tag{33}$$

where $\eta_1, \eta_2, \ldots, \eta_m$ is a set of unknown parameters. The solution of the system of Eq. 33 yields the estimates for $\eta_1, \eta_2, \ldots, \eta_m$. In our case the method of moments can also be reformulated in terms of factorial cumulants K_n that leads to considerable simplification in further mathematical derivations. To calculate theoretical factorial cumulants, it is convenient to introduce the concept of generating function. The generating function is given by [38]

$$G(\xi) = \sum_{k=0}^{\infty} \xi^k P(k), \tag{34}$$

where ξ is a trial variable and the factorial cumulants are calculated as

$$K_n = \left. \frac{d^n \ln G(\xi)}{d\xi^n} \right|_{\xi=1}. \tag{35}$$

Theoretical fluorescence factorial cumulants of PCD with out-of-focus correction can be written as follows:

$$\begin{aligned} K_1 &= \lambda T + \gamma_2 \frac{(1+F_2)}{(1+F_1)} \sum_i N_{\text{eff}\,i} q_{\text{eff}\,i} T \\ K_2 &= \gamma_2^2 \frac{(1+F_2)^2}{(1+F_1)^2} \sum_i N_{\text{eff}\,i} q_{\text{eff}\,i}^2 T^2 \\ K_n &= \gamma_2 \gamma_n \frac{(1+F_2)}{(1+F_1)^2} \sum_i N_{\text{eff}\,i} q_{\text{eff}\,i}^n T^n, \quad n = 3, 4, \ldots, \end{aligned} \tag{36}$$

All unknown parameters can be estimated from a system, where theoretical factorial cumulants (Eq. 36) are made equal to the experimentally obtained ones (Eq. 13). From a practical point of view, however, instability of higher-order factorial cumulants of PCD may result in divergence of the numerical solution. Moreover, systems of nonlinear equations are usually solved by an iterative procedure and thus require initial guesses by its own. Therefore, let us consider more simple cases leading to solutions without iterative calculations.

IG for a one-component system

According to the method of moments one has to define one equation for each estimated parameter N_{eff}, q_{eff}, F_1, F_2 and λ. However, if some parameters are known a priori and fixed to some value or simply ignored (i.e., fixed to zero), there is no need to estimate them. Therefore, one can minimize the number of higher-order cumulants needed for calculation of IG, thus increasing the efficiency and accuracy of the algorithm. The system 36, written for $n = 1,2$, $n = 1,2,3$ and $n = 1,2,3,4$ at $i = 1$ can be solved analytically. The list of obtained expressions for estimating N_{eff}, q_{eff}, F_1, and F_2 at various parameters fixing is summarized in Table 1. To get the time-independent estimates of brightness $q_{0\text{eff}}$ and number of molecules $N_{0\text{eff}}$ one has to calculate binning correction factor (*see* Eq. 3) and apply finally Eq. 32.

IG for a two-component system

To calculate IG for a two-component system, we have to define seven equations for the factorial cumulants. Although the obtained system can be solved numerically, the solution is not entirely reliable since higher-order factorial cumulants are substantially affected by noise. It is reasonable to reduce the number of equations to four and calculate IG only for brightness and number of molecules assuming that background and instrumental parameters F_1 and F_2 are known. Eq. 36 for $i = 2$ takes the form

$$\begin{aligned}
(1+F_1)(K_1-\lambda T)/\gamma_2(1+F_2)T &= N_{\text{eff}\,1}q_{\text{eff}\,1} + N_{\text{eff}\,2}q_{\text{eff}\,2}\\
(1+F_1)^2K_2\Big/\gamma_2^2(1+F_2)^2T^2 &= N_{\text{eff}\,1}q_{\text{eff}\,1}^2 + N_{\text{eff}\,2}q_{\text{eff}\,2}^2\\
(1+F_1)^2K_3/\gamma_2\gamma_3(1+F_2)T^3 &= N_{\text{eff}\,1}q_{\text{eff}\,1}^3 + N_{\text{eff}\,2}q_{\text{eff}\,2}^3\\
(1+F_1)^2K_4/\gamma_2\gamma_4(1+F_2)T^4 &= N_{\text{eff}\,1}q_{\text{eff}\,1}^4 + N_{\text{eff}\,2}q_{\text{eff}\,2}^4 .
\end{aligned} \tag{37}$$

The system 37 of nonlinear equations can be solved both analytically and numerically [23]. To rewrite the system 37 in a more compact form, we denote left-hand parts in this system as A_1, A_2, A_3, A_4. From the first equation we get an expression for estimating $N_{\text{eff}\,2}$ (*see* Eq. 18) and after substitution of Eq. 18 into the second equation of the system 37, we arrive at the third-order polynomial in respect to $q_{\text{eff}\,2}$ (*see* Eq. 15). Finally, $q_{\text{eff}\,1}$ and $N_{\text{eff}\,1}$ are calculated by Eq. 19. If the discriminant of the polynomial has a positive value, a real-valued analytical solution is available [23]. If the discriminant of the polynomial is negative, two or three real roots are available. They can be found numerically by seeking the roots of the polynomial.

The described method of IG generation can be also used independently for a quick estimation of brightness and concentrations.

3. *Relation between brightness in FCS and PCH*
Although B_0 can be safely set to unity when no correction is applied, the correction in the form of Eq. 31 makes B_0 and therefore q_{eff} a function of correction parameters F_n. Let us write the theoretical factorial cumulants of a one-component PCD without the out-of-focus correction:

$$\begin{aligned} K_1 &= \lambda T + \gamma_2 \sum_i N_{\text{eff}\,i} q_i T \\ K_k &= \gamma_2 \gamma_n \sum_i N_{\text{eff}\,i} q_i^k T^k, \quad k = 2, 3, \ldots \end{aligned} \tag{38}$$

The first two equations of Eqs. 38 and 36 yield the same expression for estimating N_{eff}

$$N_{\text{eff}} = (K_1 - \lambda T)^2 / K_2. \tag{39}$$

However the estimators of brightness are different

$$q = \frac{2\sqrt{2} K_2}{(K_1 - \lambda T) T}, \qquad q_{\text{eff}} = \frac{2\sqrt{2}(1 + F_1) K_2}{(1 + F_2)(K_1 - \lambda T) T} \tag{40}$$

Therefore, when a correction is applied (F_1, $F_2 \neq 0$), the estimated brightness represents the so-called effective or apparent brightness, which must be recalculated into the "true" one

$$q = \frac{(1 + F_2)}{(1 + F_1)} q_{\text{eff}}. \tag{41}$$

While performing FCS and PCH on the same data, one usually likes to relate brightness calculated from the average intensity $<I>$ and estimated number of molecules to the brightness obtained from PCH. From the expression for the first factorial cumulant K_1 (*see* Eq. 36), we derive

$$< I > = \frac{K_1}{T} = \lambda + \gamma_2 \frac{(1 + F_2)}{(1 + F_1)} \sum_i N_{\text{eff}\,i} q_{\text{eff}\,i}. \tag{42}$$

The expression for the first factorial cumulant does not change its form, if we replace N_{eff} and q_{eff} by their time-independent variants $N_{0\text{eff}}$ and $q_{0\text{eff}}$ (because $B_2(T) = 1$ for the first cumulant). Therefore, for a one-component model without background, one obtains $< I >= \gamma_2 (1 + F_2)\ N_{0\,\text{eff}} q_{0\,\text{eff}} / (1 + F_1)$. Since the number of molecules in FCS does not depend on time, N_{FCS} is equal to $N_{0\text{eff}}$ and

$$q_{\text{FCS}} = < I > / N_{0\,\text{eff}} = \gamma_2 (1 + F_2) q_{0\,\text{eff}} / (1 + F_1). \tag{43}$$

4. *Global χ^2 criterion*
Global analysis of experimental data obeying different functional forms may result in overestimation (or underestimation) of some model parameters, if appropriate weighting factors are

not applied to each data point. This is especially important when the number of data points in these functions is quite different, for instance, the ACF usually has 175 experimental data points versus only 10–20 data points in the PCD. Such difference in number of data points leads to a significant difference in the number of degrees of freedom (calculated as number of data points minus number of fit parameters minus one) corresponding to each analyzed curve. Thus, the standard global χ^2 criterion [39] becomes relatively insensitive to small deviations between the measured and model-generated curves that have lower number of data points. To avoid this problem it is necessary to take into account the specific weight of each individual curve that participates in the global analysis. It can be done, if χ^2 is modified, in the following way: [33]

$$\chi^2_{\text{gl mod}} = \frac{N - m - M}{M(N - m + M^{\text{gr}} - 1)} \times \sum_{i=1}^{M} \left(\frac{1}{n_i - m_i - 1} \sum_{j=1}^{n_i} \frac{\left(x_{ij} - F_{ij}^{\text{th}}\right)^2}{\sigma_{ij}^2} \right), \tag{44}$$

where $M^{\text{gr}} = \sum_{i=1}^{M} m_i^{\text{lnk}} - m^{\text{gr}}$, x_{ij}, and σ_{ij} are the measured value and the standard deviation of the ith experimental data point in the jth measured curve, and F_{ij}^{th} is the model-generated value for this point; M is the number of globally analyzed curves; n_i is the number of points in the ith curve; m_i and m_i^{lnk} is the number of free and linked parameters in the ith model, respectively; m^{gr} is the number of parameter groups (sets of linked parameters), $N = \sum_{i=1}^{M} n_i$, $m = \sum_{i=1}^{M} m_i$. As follows from Eq. 44, the contribution of each analyzed curve to the value of the global χ^2 is made equal by dividing the sum in brackets by the corresponding number of degrees of freedom (thus obtaining the local χ^2) and finally multiplying the total sum of the local χ^2 by the average number of degrees of freedom $(N - m - M)/M = \sum_{i=1}^{M} (n_i - m_i - 1)/M$. In case of equal number of degrees of freedom in each model ($n_1 = \ldots = n_M$; $m_1 = \ldots = m_M$), Eq. 25 reduces correctly to the standard global χ^2 criterion [39]:

$$\chi^2_{\text{gl}} = \frac{1}{(N - m + M^{\text{gr}} - 1)} \sum_{i=1}^{M} \sum_{j=1}^{n_i} \frac{\left(x_{ij} - F_{ij}^{\text{th}}\right)^2}{\sigma_{ij}^2}. \tag{45}$$

References

1. Magde D, Elson E, Webb WW (1972) Thermodynamic fluctuations in a reaction system: measurement by fluorescence correlation spectroscopy. Phys Rev Lett 29(11):705–708
2. Elson EL, Magde D (1974) Fluorescence correlation spectroscopy. I Conceptual basis and theory. Biopolymers 13(1):29–61
3. Magde D, Elson EL, Webb WW (1974) Fluorescence correlation spectroscopy. II. An experimental realization. Biopolymers 13 (1):29–61. doi:10.1002/bip.1974.360130103
4. Krichevsky O, Bonnet G (2002) Fluorescence correlation spectroscopy: the technique and its applications. Rep Prog Phys 65:251–297
5. Thompson NL, Lieto AM, Allen NW (2002) Recent advances in fluorescence correlation spectroscopy. Curr Opin Struct Biol 12 (5):634–641
6. Haustein E, Schwille P (2007) Fluorescence correlation spectroscopy: novel variations of an established technique. Annu Rev Biophys Biomol Struct 36:151–169. doi:10.1146/annurev.biophys.36.040306.132612
7. Rigler R, Elson E (eds) (2001) Fluorescence correlation spectroscopy. Theory and applications. Springer, Berlin
8. Widengren J, Mets U, Rigler R (1995) Fluorescence correlation spectroscopy of triplet states in solution: a theoretical and experimental study. J Phys Chem 99:13368–13379
9. Chen Y, Müller JD, So PT, Gratton E (1999) The photon counting histogram in fluorescence fluctuation spectroscopy. Biophys J 77 (1):553–567
10. Chen Y, Tekmen M, Hillesheim L, Skinner J, Wu B, Müller JD (2005) Dual-color photon-counting histogram. Biophys J 88(3):2177–2192. doi:10.1529/biophysj.104.048413
11. Kask P, Palo K, Ullmann D, Gall K (1999) Fluorescence-intensity distribution analysis and its application in biomolecular detection technology. Proc Natl Acad Sci U S A 96 (24):13756–13761
12. Kask P, Palo K, Fay N, Brand L, Mets U, Ullmann D, Jungmann J, Pschorr J, Gall K (2000) Two-dimensional fluorescence intensity distribution analysis: theory and applications. Biophys J 78(4):1703–1713
13. Hess ST, Webb WW (2002) Focal volume optics and experimental artifacts in confocal fluorescence correlation spectroscopy. Biophys J 83(4):2300–2317
14. Hillesheim LN, Müller JD (2003) The photon counting histogram in fluorescence fluctuation spectroscopy with non-ideal photodetectors. Biophys J 85(3):1948–1958
15. Enderlein J, Gregor I, Patra D, Dertinger T, Kaupp UB (2005) Performance of fluorescence correlation spectroscopy for measuring diffusion and concentration. Chemphyschem 6 (11):2324–2336
16. Gregor I, Patra D, Enderlein J (2005) Optical saturation in fluorescence correlation spectroscopy under continuous-wave and pulsed excitation. Chemphyschem 6(1):164–170. doi:10.1002/cphc.200400319
17. Perroud TD, Huang B, Wallace MI, Zare RN (2003) Photon counting histogram for one-photon excitation. Chemphyschem 4 (10):1121–1123. doi:10.1002/cphc.200300824
18. Huang B, Perroud TD, Richard N (2004) Photon counting histogram: one-photon excitation. Chemphyschem 5:1523–1531
19. Palo K, Metz U, Jager S, Kask P, Gall K (2000) Fluorescence intensity multiple distributions analysis: concurrent determination of diffusion times and molecular brightness. Biophys J 79 (6):2858–2866
20. Perroud TD, Huang B, Zare RN (2005) Effect of bin time on the photon counting histogram for one-photon excitation. Chemphyschem 6 (5):905–912
21. Palo K, Mets U, Loorits V, Kask P (2006) Calculation of photon count number distributions via master equations. Biophys J 90:2179–2191
22. Gopich IV, Szabo A (2005) Photon counting histograms for diffusive fluorophores. J Phys Chem B 109:17683–17688
23. Skakun VV, Novikov EG, Apanasovich VV, Tanke HJ, Deelder AM, Mayboroda OA (2006) Initial guesses generation for fluorescence intensity distribution analysis. Eur Biophys J 35(5):410–423. doi:10.1007/s00249-006-0048-8
24. Visser AJWG, Laptenok SP, Visser NV, van Hoek A, Birch DJS, Brochon JC, Borst JW (2010) Time-resolved FRET fluorescence spectroscopy of visible fluorescent protein pairs. Eur Biophys J 39:241–253. doi:10.1007/s00249-009-0528-8
25. Hink MA, Shah K, Russinova E, de Vries SC, Visser AJWG (2008) Fluorescence fluctuation analysis of *Arabidopsis thaliana* somatic embryogenesis receptor-like kinase and brassinosteroid insensitive 1 receptor oligomerization. Biophys J 94(3):1052–1062. doi:10.1529/biophysj.107.112003

26. Hink MA, Borst JW, Visser AJWG (2003) Fluorescence correlation spectroscopy of GFP fusion proteins in living plant cells. Methods Enzymol 361:93–112
27. Weisshart K, Jüngel V, Briddon SJ (2004) The LSM 510 META - ConfoCor 2 system: an integrated imaging and spectroscopic platform for single-molecule detection. Curr Pharm Biotechnol 5:135–154
28. Marquardt DW (1963) An algorithm for least-squares estimation of non-linear parameters. J Soc Ind Appl Math 11:431–441
29. Skakun VV, Hink MA, Digris AV, Engel R, Novikov EG, Apanasovich VV, Visser AJ (2005) Global analysis of fluorescence fluctuation data. Eur Biophys J 34(4):323–334
30. Meng F, Ma H (2006) A comparison between photon counting histogram and fluorescence intensity distribution analysis. J Phys Chem B 110(51):25716–25720
31. Lau HT (1995) A numerical library in C for scientists and engineers, Symbolic and numeric computation series. CRC Press, Boca Raton, FL
32. Press WH, Teukolsky SA, Vetterling WT, Flannery BP (1992) Numerical recipes in C: the art of scientific computing, 2nd edn. Cambridge University Press, New York, NY
33. Skakun VV, Engel R, Digris AV, Borst JW, Visser AJ (2011) Global analysis of autocorrelation functions and photon counting distributions. Front Biosci (Elite Ed) 3:489–505, 264 [pii]
34. Bevington PR, Robinson DK (2003) Data reduction and error analysis for the physical sciences, 3rd edn. McGraw-Hill, New York, NY
35. Wohland T, Rigler R, Vogel H (2001) The standard deviation in fluorescence correlation spectroscopy. Biophys J 80(6):2987–2999. doi:10.1016/S0006-3495(01)76264-9, S0006-3495(01)76264-9 [pii]
36. Malikova NP, Visser NV, van Hoek A, Skakun VV, Vysotski ES, Lee J, Visser AJ (2011) Green-fluorescent protein from the bioluminescent jellyfish *Clytia gregaria* is an obligate dimer and does not form a stable complex with the Ca(2+)-discharged photoprotein clytin. Biochemistry 50(20):4232–4241. doi:10.1021/bi101671p
37. Dross N, Spriet C, Zwerger M, Muller G, Waldeck W, Langowski J (2009) Mapping eGFP oligomer mobility in living cell nuclei. PLoS One 4(4):e5041. doi:10.1371/journal.pone.0005041
38. Korn GA, Korn TM (1968) Mathematical handbook for scientists and engineers. Definitions, theorems and formulas for reference and review. Second, enlarged and revised edition. McGraw-Hill Book Company, New York, NY
39. Beechem JM, Gratton E, Ameloot M, Knutson JR, Brand L (1991) Analysis of fluorescence intensity and anisotropy decay data: second generation theory and programs. In: Lakowicz JR (ed) Topics in fluorescence spectroscopy, vol 2. Plenum Press, New York, NY, pp 241–305
40. Johnson ML, Faunt LM (1992) Parameter estimation by least-squares methods. Methods Enzymol 210:1–37